

Associated production of heavy Higgs bosons with a $b\bar{b}$ pair in the Nonholomorphic MSSM and LHC searches

Utpal Chattopadhyay,^a Aresh Krishna Datta,^b Samadrita Mukherjee,^c Abhaya Kumar Swain^d

^a*School of Physical Sciences, Indian Association for the Cultivation of Science,
2A & B Raja S.C. Mullick Road, Jadavpur, Kolkata 700 032, India*

^b*Harish-Chandra Research Institute, HBNI, Chhatnag Road, Jhusi, Allahabad-211019, India*

^c*Department of Theoretical Physics, Tata Institute of Fundamental Research, 1 Homi Bhabha Road, Colaba, Mumbai 400005, India*

^d*School of Physics and Institute for Collider Particle Physics, University of the Witwatersrand, Johannesburg, Wits 2050, South Africa*

E-mail: tpuc@iacs.res.in, asesh@hri.res.in, samadrita.mukherjee@tifr.res.in,
abhaya.kumar.swain@cern.ch

ABSTRACT: In the NonHolomorphic Supersymmetric Standard Model (NHSSM), the Yukawa couplings of the bottom quark (y_b) and the tau lepton (y_τ) might receive substantial supersymmetric (SUSY) radiative corrections which have prominent dependencies on the NHSSM-specific trilinear soft parameters, A'_b and A'_τ , respectively, in addition to their well-known dependence on $\tan\beta$ as is already present in the Minimal SUSY Standard Model (MSSM). We study to what extent these could affect the production cross sections of the heavy Higgs bosons (H and A) in association with a pair of b -quarks and their decay branching ratios, in particular, to a $\tau\bar{\tau}$ pair and compare them with those obtained in the MSSM. Requiring compliance with the recently observed upper bounds on the product of their total cross section and the branching ratio to $\tau\bar{\tau}$ at the 13 TeV run of the Large Hadron Collider (LHC), with data worth 139 fb^{-1} , results in an altered exclusion region in the customary $m_A - \tan\beta$ plane in the framework of the NHSSM when compared to what is derived by the LHC experiments within an MSSM setup. Such alterations are estimated to be pronounced only for large $\tan\beta$ (≥ 40) and for large, negative A'_b when one finds a reinforced exclusion of the $m_A - \tan\beta$ plane with an excluded m_A value larger by $\approx 350 \text{ GeV}$, compared to the MSSM case, at $\tan\beta = 60$. On the other hand, the maximum relaxation in m_A , for a similarly large but positive A'_b , barely exceeds $\approx 100 \text{ GeV}$ as a result of complementary variations in production cross sections and decay branching fractions of the heavy, neutral Higgs bosons.

KEYWORDS: Beyond Standard Model, Supersymmetry Phenomenology, Collider Physics

Contents

1	Introduction	1
2	The theoretical setup	3
2.1	The NHSSM scenario	4
2.2	Radiative corrections to y_b and y_τ	4
2.3	The Higgs sector	6
3	Results	7
3.1	Variations of $bb\Phi$ and $\tau\tau\Phi$ interaction strengths	9
3.2	Decays of the heavier neutral Higgs bosons	13
3.3	Production of heavier neutral Higgs bosons (H, A) with a bottom quark pair	14
3.4	Constraining $m_A - \tan\beta$ plane: NHSSM vis-a-vis LHC exclusion (in the MSSM)	17
4	Conclusions	19

1 Introduction

Ever since its discovery at the Large Hadron Collider (LHC) the properties of ‘the’ Higgs boson are being probed in minute details thanks to the increasing volume of the accumulated data. While its mass, which is not predicted by the theory, is being estimated with an ever-increasing precision, various couplings of the Higgs boson are being measured with even greater accuracy. It is now known that whereas its couplings to the gauge bosons agree with their predictions from the Standard Model (SM) at the $\sim 5\%$ level, the same with the fermions from the third generation, to date, could attain compatibility with the SM only at the level of 15-20% [1].

The latter set of couplings are the Yukawa couplings (y_b, y_t and y_τ) that are proportional to the respective fermion (bottom, top and tau) masses. These are rather special in the sense that, when compared to the minuscule ones for the light fermions from the first two generations, these are much larger. In addition, the magnitudes of such couplings could also be sensitive to scenarios beyond the SM, the implications of which could well transcend the exclusive domain of particle physics by possibly influencing the physics of the early Universe. Direct experimental probes to such couplings thus have to be of paramount importance.

It is appreciated that any such fundamental coupling of a given excitation, when could appear both in its production and decay, should be determined by studying them in tandem to reduce the involved uncertainties in its estimation. In the current context of the SM(-like) Higgs boson (h_{SM}), such a combined approach is inherently unavoidable given its production cross section at the LHC in any relevant mode and its decays (branching fractions) could get to be largely interlaced and hence the couplings are not independently extricable [2]. As for the Yukawa couplings, each of y_t and y_b might play role in both production and decay of the Higgs boson. However, as pointed out in reference [2], the possibility of efficient extraction of y_b in the decay $h_{\text{SM}} \rightarrow b\bar{b}$ is marred by

several issues even though this has the largest branching fraction. A priori, a better sensitivity to y_b has been expected in the associated $h_{\text{SM}}b\bar{b}$ production mode notwithstanding the large irreducible background that it attracts. This is since such a mode is much less encumbered with theoretical assumptions when compared to working with the decay branching fraction $\text{BR}[h_{\text{SM}} \rightarrow b\bar{b}]$ which depends on to what extent h_{SM} decays to other modes and can be highly model-dependent. However, while the LHC experiments are yet to take a dedicated look into the $h_{\text{SM}}b\bar{b}$ production process (which has a cross section similar to that of $h_{\text{SM}}t\bar{t}$ production that has already been studied by the experiments), a recent study [3] has cast a shadow on its prospects.

Under the circumstances, studying productions of various Higgs bosons, possibly heavier than h_{SM} , in association with a $b\bar{b}$ -pair in scenarios with extended Higgs sector assumes a heightened significance. Extensions of the SM endowed with two Higgs doublets, of which the Minimal Supersymmetric extension of the SM (MSSM) is a popular example, are in immediate reference here. Such production modes could be the direct probes to such scenarios. This is since in these scenarios y_b could get significantly enhanced for large values of $\tan\beta (= \frac{v_u}{v_d})$, the ratio of the vacuum expectation values (*vev's*), v_u and v_d , of the neutral components of the two Higgs doublets. In addition, the interaction vertices of Higgs bosons and a $b\bar{b}$ pair have an additional $1/\cos\beta$ dependence which lead to their enhanced interaction strengths for larger values of $\tan\beta$. Even then, it has been observed that unless y_b gets significantly enhanced in such new physics scenarios, a production process like $h_{\text{SM}}b\bar{b}$ is unlikely to be useful for the purpose. It has been recently pointed out [3] that such an enhancement in y_b is strongly disfavored by the current measurements of the $h_{\text{SM}} \rightarrow b\bar{b}$ decay. This is consistent with the implications of the recent bounds on the m_A - $\tan\beta$ plane [4–6], m_A being the mass of the CP -odd Higgs boson of the MSSM scenario, which indicates that the $h_{\text{SM}}b\bar{b}$ coupling may not be reinforced enough even when y_b is significantly enhanced because of a suppressed mixing between the two CP -even Higgs states of the MSSM.

In this backdrop, a renewed impetus for carrying out such studies can now be drawn from the recent discourses of an otherwise MSSM scenario but for the presence of additional ‘nonholomorphic’ soft terms in its Lagrangian which goes by the name of Nonholomorphic Supersymmetric Standard Model (NHSSM)[7–16]. It is further known that the presence of generic nonholomorphic terms like $A'_f\phi^*\phi$ could have important implications [17]. In particular, the nonholomorphic trilinear soft term from the bottom quark sector involving A'_b and A'_τ might play important roles in the phenomenology of the NHSSM as these could radiatively alter the magnitudes of y_b and y_τ , respectively [18], over and above what is induced by $\tan\beta$ in the MSSM [19–24]. Even then, the couplings $h_{\text{SM}}b\bar{b}/\tau\bar{\tau}$ remain suppressed because of the reason mentioned in the previous paragraph. In a complementary way, the heavier Higgs bosons of the scenario are well-poised to receive the maximal benefit of the suppressed Higgs mixing angle and hence their productions in association with a $b\bar{b}$ pair might emerge to be more potential probes to y_b . However, the LHC bound mentioned earlier that is obtained assuming the MSSM framework is expected to be sensitive to the parameter(s) (like A'_b) of the NHSSM. Hence a recast of the bound in the NHSSM scenario would be necessary before drawing a conclusion.

Radiatively corrected y_b and y_τ in the NHSSM scenario are expected to affect the constraints derived in the MSSM framework by the LHC experiments on the heavy Higgs boson sector in the form of an exclusion in the $m_A - \tan\beta$ plane. This is since these studies search for heavier Higgs bosons in their productions in association with b -quark(s), i.e., $pp \rightarrow b\bar{b}H/A$ [4–6], btH^\pm

[25, 26], and their subsequent decays to τ -leptons (and to top quarks, in the case of H^\pm), i.e., $H, A \rightarrow \tau\bar{\tau}$, $H^\pm \rightarrow \tau\nu_\tau$ [25], [26]. However, an understanding of the extents to which y_b and y_τ could actually influence the proceedings requires a somewhat detailed analysis which we take up duly in this work. As for the H^\pm states, their searches at the LHC, as yet, could only set much weaker exclusions on the $m_A - \tan\beta$ plane when compared to those from the searches of the H/A , except for rather low values of $\tan\beta$ ($\lesssim 2$) which are anyway not so relevant for the phenomenology of the latter states that we are interested in. Hence we do not discuss the related phenomenology of the H^\pm states separately in the present work.

Production processes of Higgs bosons in association with bottom squarks (\tilde{b}) also involve y_b and hence are, a priori, in context. However, we find that given the current ATLAS lower bounds on the mass of the lighter sbottom (\tilde{b}_1) [27], the maximum $\sigma_{(pp \rightarrow \tilde{b}_1 \tilde{b}_1^* H)}$ obtainable over the NHSSM parameter space for a relatively light ‘ H ’ state is smaller by quite a few orders when compared to $\sigma_{(pp \rightarrow b\bar{b}H)}$ for the same m_H . For our purposes, we add to the latter the contribution $\sigma_{(pp \rightarrow b\bar{b}A)}$ where $m_A \simeq m_H$. In contrast, note that $\sigma_{(pp \rightarrow \tilde{b}_1 \tilde{b}_1^* A)}$ vanishes since the vertex $A\tilde{b}_1\tilde{b}_1$ is absent [28] and $\sigma_{(pp \rightarrow \tilde{b}_1 \tilde{b}_2^* A + \text{c.c.})}$ is further suppressed due to a more massive \tilde{b}_2 in the final state. Thus, the combined rate for H, A production in association with a pair of sbottoms is way too small to be sensitive to the contemporary runs of the LHC. Hence we do not consider those processes further. We are then set free to consider much larger soft SUSY breaking masses for the sbottoms (as well as, for the staus), $m_{\tilde{b},\tilde{\tau}}$. This, in turn, allows us to study a wider range of values for the phenomenologically interesting NHSSM parameters like $A'_{b,\tau}$ ($\lesssim m_{\tilde{b},\tilde{\tau}}$) without running the risk of encountering a tachyonic spectrum or a charge and color breaking (CCB) minimum in the scalar potential of the theory or jeopardizing the stability of the electroweak vacuum [29]. Henceforth, we refer to these issues collectively as the CCB problem.

The paper is organized as follows. In section 2 we outline the theoretical setup of the NHSSM scenario under study with an emphasis on how the same could provide additional radiative corrections to running $y_{b,\tau}$ (in the presence of a nonvanishing $A'_{b,\tau}$) over and above the ones found in the MSSM ($\tan\beta$ -enhancement)) and how these new effects modify the couplings of the neutral Higgs bosons to a b -quark or a τ -lepton pair. Section 3 is devoted to a detailed study of decays of the heavier neutral Higgs bosons, ‘ H ’ and ‘ A ’, to a $b\bar{b}$ and a $\tau\bar{\tau}$ pair (the only accessible final states, following relevant experimental studies) for varying $\tan\beta$ and $A'_{b,\tau}$. This is followed by a study of similar variations of the combined cross section for the associated $b\bar{b}\Phi$ ($\Phi \equiv H, A$) productions at the 13 TeV LHC where we discuss briefly some involved theoretical considerations that go into obtaining a state-of-the-art, precise estimate of these cross sections. The variation of the quantity $\sigma_{(pp \rightarrow b\bar{b}H,A)} \times \text{BR}[H, A \rightarrow \tau\bar{\tau}]$ is then studied in detail over the relevant parameter space of the NHSSM and then confronted by the experimental bound on the same. The results are then recast on the $m_A - \tan\beta$ plane with $A'_{b,\tau}$ as parameters to find the ways in which the exclusion contour obtained by the LHC experiments gets modified in the NHSSM scenario. In section 4 we conclude.

2 The theoretical setup

In this section, we first briefly discuss the ingredients of the NHSSM scenario which can be seen as an augmented version of the much popular MSSM scenario. Given that the bottom Yukawa coupling is central to the present study, we then outline how the radiative correction to the running

mass y_b (m_b) gets modified in the NHSSM scenario when compared to the MSSM contribution to the same. Finally, we touch upon the structure of the Higgs sector which is no different from that in the MSSM scenario. We point out a few of its salient features that are in the direct context of the present study.

2.1 The NHSSM scenario

Considering the fact that nonholomorphic terms (*e.g.*, $\phi^2\phi^*$ and $\psi\psi$) in the Lagrangian [8, 17] could have an impact on phenomenological observables, we include such terms as electroweak scale input parameters so that they can have strengths similar to that of the other soft terms already present in the MSSM.

The parts of the Lagrangian containing the NH terms are given by,

$$-\mathcal{L}'_{soft}{}^{\phi^2\phi^*} = \tilde{q} \cdot h_d^* \mathbf{A}'_u \tilde{u}^* + \tilde{q} \cdot h_u^* \mathbf{A}'_d \tilde{d}^* + \tilde{\ell} \cdot h_u^* \mathbf{A}'_\ell \tilde{e}^* + \text{h.c.}, \quad (2.1)$$

$$-\mathcal{L}'_{soft}{}^{\psi\psi} = \mu' \tilde{h}_u \cdot \tilde{h}_d, \quad (2.2)$$

where $A'_{u,d,\ell}$ are the NH soft trilinear parameters corresponding to the up, down and lepton sectors, respectively. We note that the Higgs field associated with the up and down types of squarks are reversed as compared to the holomorphic trilinear terms to assign correct hypercharges. μ' is the soft higgsino mass parameter.

The presence of the NH soft trilinear terms containing A'_f modifies the off-diagonal terms of the tree-level sfermion mass-squared matrices of the MSSM. Thus, in the NHSSM, the modified off-diagonal elements of the tree-level mass-squared matrices have the generic form $-m_f[A_f - (\mu + A'_f)r_\beta]$ for the up-type squark ($r_\beta = \cot\beta$) and down-type squark/stau ($r_\beta = \tan\beta$) mass-squared matrices [17]. Here m_f is the mass of the corresponding fermion, A_f are the corresponding soft trilinear parameters that appear in the scalar potential, while ' μ ' is the SUSY conserving holomorphic higgsino mass parameter that appears in the superpotential. Unlike in the MSSM, contributions from the trilinear (NH) soft parameters (A'_f) arise through their products with either $\cot\beta$ (for the *up* quark sector) or $\tan\beta$ (for the *down*-quark and the charged lepton sectors). Hence such contributions could get enhanced for the bottom and tau sectors when $\tan\beta$ is large. In turn, any phenomenological observable which involves a chiral mixing of sfermions would be affected by such NH parameters.

As for the neutralino and the chargino (the electroweakinos) sectors, those are affected at the tree level in the presence of NH μ' terms. The higgsino entries of the neutralino and the chargino mass matrices undergo the modification $\mu \rightarrow \mu + \mu'$ [17].

2.2 Radiative corrections to y_b and y_τ

An important implication of the presence of NH trilinear soft terms involving A'_f (A'_b and A'_τ) in the NHSSM Lagrangian is that those could influence the radiative corrections to the down-type Yukawa couplings, y_b and y_τ , thus modifying their tree-level relations to m_b and m_τ , respectively. These are over and above their dependencies on $\tan\beta$ that are already present in the MSSM.

At one-loop level, the principal MSSM contributions to y_b arise from the gluino-sbottom ($\tilde{g}-\tilde{b}_i$) loop and the chargino-stop ($\chi_i^\pm - \tilde{t}$) loop [19–24]. On the other hand, in the NHSSM where H_u is also associated with the down type squarks (and sleptons) in the trilinear soft interactions, one can

have an extra $\tilde{g} - \tilde{b}$ contribution with a factor $A'_b y_b$ showing up at the $\tilde{b}_L - H_u^* - \tilde{b}_R$ vertex. Besides, there is a neutralino-sbottom ($\chi_i^0 - \tilde{b}$) loop contribution with the same factor $A'_b y_b$ appearing at the trilinear scalar vertex and a factor of y_b^2 coming from the other two vertices having $\tilde{b}_L \tilde{b}_R \chi^0$ interactions with their origins in the superpotential [18]. At one-loop level, the modified relation between m_b and y_b in the NHSSM (which is identical in appearance to that in the MSSM)¹ and hence the radiatively-corrected expression for y_b is given by

$$m_b = \frac{y_b v_d}{\sqrt{2}}(1 + \Delta_b) \quad \Longrightarrow \quad y_b = \frac{\sqrt{2}m_b}{v_d(1 + \Delta_b)}, \quad (2.3)$$

where Δ_b now contains the NHSSM contributions, in addition to the MSSM ones and is given by

$$\begin{aligned} \Delta_b = & \frac{y_{t_{\text{SM}}}^2}{16\pi^2} \mu A_t I(m_{\tilde{t}_1}^2, m_{\tilde{t}_2}^2, (\mu + \mu')^2) \tan \beta + \frac{2\alpha_s}{3\pi} m_{\tilde{g}}(\mu + A'_b) I(m_{\tilde{b}_1}^2, m_{\tilde{b}_2}^2, m_{\tilde{g}}^2) \tan \beta \\ & + \frac{y_{\tilde{b}_{\text{SM}}}^2}{16\pi^2} \mu(\mu + A'_b) I(m_{\tilde{b}_1}^2, m_{\tilde{b}_2}^2, (\mu + \mu')^2) \tan \beta, \end{aligned} \quad (2.4)$$

where the characteristic loop (integral) function $I(a, b, c)$ involving loop-momentum ‘ u ’ and squared masses a, b, c of the three propagating states in the loop is given by [19]

$$I(a, b, c) = \int_0^\infty \frac{udu}{(u+a)(u+b)(u+c)} = \frac{ab \ln(a/b) + bc \ln(b/c) + ca \ln(c/a)}{(a-b)(b-c)(a-c)}, \quad (2.5)$$

and α_s is the strong coupling constant and A_t and $m_{\tilde{g}}$ are the soft SUSY breaking trilinear coupling of the top squarks to the up-type Higgs field and the mass of the gluino, respectively. To make a generic numerical sense of this involved function, it may be noted that the same can be parametrized as $I(a, b, c) = K_I/a_{\text{max}}$ [21] where $a_{\text{max}} = \max(a, b, c)$ is the maximum of the three squared masses appearing there and $K_I \simeq 0.5 - 0.9$ in the absence of a large hierarchy between these masses.²

The corresponding corrections to y_τ (m_τ) are expected to come from $\chi_i^\pm - \tilde{\nu}_\tau$ and $\chi_i^0 - \tilde{\tau}$ loops only and are driven by A'_τ and $\tan \beta$. Thus, the relations in equations 2.3 and 2.4 can be used for the modified expression for m_τ (y_τ) by dropping the α_s -dependent gluino contribution straightaway and replacing all bottom(top)-flavor related parameters by their leptonic ($\tau(\nu_\tau)$) counterparts. As a result, the corresponding first term which would represent the contribution from the $\chi_i^\pm - \tilde{\nu}_\tau$ loop and would go as the (vanishing) neutrino Yukawa coupling ($y_t \rightarrow y_{\nu_\tau}$) also drops out leading to

$$\Delta_\tau = \frac{y_{\tau_{\text{SM}}}^2}{16\pi^2} \mu(\mu + A'_\tau) I(m_{\tilde{\tau}_1}^2, m_{\tilde{\tau}_2}^2, (\mu + \mu')^2) \tan \beta. \quad (2.6)$$

The modified relation between m_τ and y_τ and hence the expression for corrected y_τ are given by

$$m_\tau = \frac{y_\tau v_d}{\sqrt{2}}(1 + \Delta_\tau) \quad \Longrightarrow \quad y_\tau = \frac{\sqrt{2}m_\tau}{v_d(1 + \Delta_\tau)}. \quad (2.7)$$

As can be seen from equations 2.3 – 2.7, the one-loop corrected $y_{b(\tau)}$ not only has an explicit direct dependence on $\tan \beta$ as is the case in the MSSM but also has an additional dependence on

¹References [30–32] contain detailed analysis on the effective Higgs boson vertices that involve nonholomorphic A'_f terms in SUSY-QCD and electroweak corrections to m_f (y_f).

²The limiting values of K_I ($=0.5$ (1)) are obtained by carrying out the shown integration with one (two) of the masses vanishing.

$A'_b(A'_\tau)$ (via the quantity $\mu + A'_b$ ($\mu + A'_\tau$)) in the NHSSM which is roughly on the same footing as $\tan\beta$ when ‘ μ ’ is not too large. Also, note that in the NHSSM, for a non-vanishing μ' , the loop function $I(a, b, c)$ in equation 2.4 takes $(\mu + \mu')^2$ in its argument instead of μ^2 that appears in the MSSM. Furthermore, it is clear from the expressions in equations 2.3 and 2.7 that one expects enhancements (suppressions) in $y_{b,\tau}$ for $\Delta_{b,\tau} < 0$ (> 0).

2.3 The Higgs sector

As mentioned earlier, the Higgs sector of the NHSSM is structurally similar to that of the MSSM having two complex Higgs doublets of opposite hypercharges thus leading to five physical Higgs states once the electroweak symmetry gets broken. These are the two CP -even Higgs states, ‘ h ’ and ‘ H ’, of which the lighter one (h) is SM-like ($h \equiv h_{\text{SM}}$); a CP -odd one, ‘ A ’, and two charged Higgs states, H^\pm .

At the tree level, the masses of these physical states and their couplings with the SM fermions and the gauge bosons depend only on two free parameters. These are conventionally chosen to be the ratio of the vacuum expectation values (*vevs*) of the neutral components of the two Higgs doublets, viz., $\tan\beta = \frac{v_2}{v_1}$ and the mass of the physical CP -odd neutral Higgs state, m_A [33]. Thus, the masses of the other four Higgs states, at the tree level, are given by

$$m_{h,H}^2 = \frac{1}{2} \left[m_A^2 + m_Z^2 \mp \sqrt{(m_A^2 + m_Z^2) - 4m_A^2 m_Z^2 \cos^2 2\beta} \right], \quad m_{H^\pm}^2 = m_A^2 + m_{W^\pm}^2, \quad (2.8)$$

where m_Z and m_{W^\pm} are the masses of the SM ‘ Z ’ and W^\pm bosons, respectively. It follows that for $m_A \gg m_Z$, $m_H \approx m_{H^\pm} \approx m_A$. When the Higgs sector conserves the CP symmetry, the physical CP -even neutral Higgs states (h, H) are obtained from their weak counterparts via the rotation [34]

$$\begin{pmatrix} H \\ h \end{pmatrix} = \begin{pmatrix} \cos\alpha & \sin\alpha \\ -\sin\alpha & \cos\alpha \end{pmatrix} \begin{pmatrix} H_1^0 \\ H_2^0 \end{pmatrix}, \quad (2.9)$$

where the Higgs mixing angle ‘ α ’ controls the interactions of these physical Higgs states with the fermions, the gauge bosons, the sfermions and the electroweakinos and is given by m_A and $\tan\beta$ as

$$\alpha = \frac{1}{2} \tan^{-1} \left(\tan 2\beta \frac{m_A^2 + m_Z^2}{m_A^2 - m_Z^2} \right) \quad \text{with} \quad -\frac{\pi}{2} \leq \alpha \leq 0. \quad (2.10)$$

The couplings of these Higgs states with the bottom quark, which are in direct reference in the present work, are given at the tree level by their MSSM expressions [33]

$$G_{hbb} = -i \frac{m_b \sin\alpha}{v \cos\beta}, \quad G_{Hbb} = i \frac{m_b \cos\alpha}{v \cos\beta}, \quad G_{Abb} = \frac{m_b}{v} \tan\beta \gamma_5, \quad (2.11)$$

where $v = \sqrt{v_u^2 + v_d^2} = 246$ GeV. In the units of the tree-level SM b -quark Yukawa coupling $y_b = \frac{im_b}{v}$, the first two couplings of equation 2.11 reduce to

$$\begin{aligned} g_{hbb} &= -\frac{\sin\alpha}{\cos\beta} = \sin(\beta - \alpha) - \tan\beta \cos(\beta - \alpha), \\ g_{Hbb} &= \frac{\cos\alpha}{\cos\beta} = \cos(\beta - \alpha) + \tan\beta \sin(\beta - \alpha). \end{aligned} \quad (2.12)$$

Thus, in the so-called decoupling limit ($m_A \gg m_Z$ and $\tan \beta \gg 1$), when $\cos(\beta - \alpha) \rightarrow 0$, $\sin(\beta - \alpha) \rightarrow 1$ and the factor γ_5 is ignored,³ one finds

$$g_{hbb} \rightarrow 1, \quad g_{Hbb} \rightarrow \tan \beta, \quad g_{Abb} = \tan \beta. \quad (2.13)$$

The bottom line is that the Hbb coupling in the decoupling limit and the Abb coupling are both enhanced by a factor of $\tan \beta$. On the other hand, the hbb coupling gets $\tan \beta$ -enhanced in the non-decoupling limit for which $m_A \gtrsim m_Z$. It suffices to mention here that, in contrast, the coupling of the Higgs bosons to the top quark(s) are generically $\tan \beta$ -suppressed (i.e., $\cot \beta$ -enhanced) and the couplings of ‘ h ’ and ‘ H ’ to top quarks have just the opposite dependencies on $\tan \beta$ when compared to the same to bottom quarks.

At this point, it is important to note that these couplings receive crucial higher-order (SUSY-QCD and SUSY-electroweak) corrections whereby the reduced couplings, for the neutral Higgs states, are given by [33]

$$\begin{aligned} g_{hbb} &\simeq -\frac{\sin \bar{\alpha}}{\cos \beta} \left[1 - \frac{\Delta_b}{1 + \Delta_b} (1 + \cot \bar{\alpha} \cot \beta) \right], \\ g_{Hbb} &\simeq \frac{\cos \bar{\alpha}}{\cos \beta} \left[1 - \frac{\Delta_b}{1 + \Delta_b} (1 - \tan \bar{\alpha} \cot \beta) \right], \\ g_{Abb} &\simeq \tan \beta \left[1 - \frac{\Delta_b}{1 + \Delta_b} \frac{1}{\sin^2 \beta} \right], \end{aligned} \quad (2.14)$$

where $\bar{\alpha}$ stands for the radiatively corrected Higgs mixing angle [33] which now includes possible NHSSM effects in addition to the ones of the MSSM origin and Δ_b is as defined in equation 2.4.

An analogous $\tan \beta$ -dependence follows for y_τ but for the absence of an α_s -driven gluino contribution to Δ_τ (as given in equation 2.6; when compared to equation Δ_b of 2.4). Thus, y_τ would be intrinsically smaller and so would be its range of variation about its nominal MSSM value when A'_τ is varied, as opposed to the range of variation of y_b under a varying A'_b . This implies that it is A'_b , rather than A'_τ , that would broadly dictate the decay branching fractions of H/A to $\tau\bar{\tau}$, the final state which the LHC experiments exploit in their search for these Higgs states in their associated productions with a $b\bar{b}$ pair [4–6].

Armed with the above knowledge of the $(H/A)b\bar{b}$, $(H/A)\tau\bar{\tau}$ couplings in the NHSSM, we now take up the study of the production of these Higgs states in association with a $b\bar{b}$ pair at the LHC and their subsequent decays to $b\bar{b}$ and $\tau\bar{\tau}$ pairs. The goal is to find out how the variation of the quantity $\sigma_{(pp \rightarrow b\bar{b}H/A)} \times \text{BR}[H/A \rightarrow \tau\bar{\tau}]$ that offers the most stringent LHC exclusion of the customary $m_A - \tan \beta$ plane differs in the NHSSM from that in the MSSM in the presence of a non-vanishing A'_b and hence the impact of the same in modifying the said exclusion region.

3 Results

In this section, we present our results by first studying the dependencies of the Yukawa couplings y_b and y_τ on the NHSSM trilinear parameters A'_b and A'_τ , respectively, and $\tan \beta$. While for the productions of ‘ H ’ and ‘ A ’ in association with a $b\bar{b}$ pair, variations of both y_b and $\tan \beta$ play

³For a massive b -quark, the process of dimensionally regularizing the calculation is somewhat involved given that the Dirac matrix γ_5 is a four-dimensional construct. The resulting effects of a finite m_b are small $\sim \mathcal{O}\left(\frac{m_b^2}{m_A^2}\right)$ [35].

Parameters	MSSM	NHSSM
μ (GeV)	500	
M_1, M_2, M_3 (TeV)	2, 2, 3	
$\tan \beta$	[5 : 60]	
m_A (TeV)	[0.35 : 3]	
$m_{\tilde{q}}, m_{\tilde{\ell}}$ (TeV)	3	
$A_{t,b,\tau}$ (TeV)	-2.7, 0, 0	
μ' (TeV)	–	1.5
A'_t (TeV)	–	0
A'_b, A'_τ (TeV)	–	[-3 : 3]

Table 1. Fixed values and ranges adopted for various low scale input SUSY parameters.

major roles, their decays, are expected to be further governed by y_τ . A study on the decays of the heavy Higgs bosons of the NHSSM follows. We then touch upon some important theoretical issues in the calculation of the cross section for the process $pp \rightarrow b\bar{b}H/A$ at the LHC energies before describing our approach of calculating the same. All these are aimed to find out how the nontrivial dependencies of various (Yukawa) couplings of such Higgs bosons affect the sensitivity of the LHC to these states when produced in association with a pair of bottom quarks. This then prompts us to examine to what extent the constraints from the latest LHC searches in the said mode could get relaxed or further strengthened in the NHSSM scenario.

To focus on the NHSSM-specific sector of the parameter space, in particular, the part that involves the trilinear coupling parameters A'_b and A'_τ and which could affect the phenomenology of the bottom quark and tau lepton, we fix all other SUSY parameters to their suitable values such that various important bounds from the LHC experiments are complied with and the observed properties of the SM-like Higgs bosons could be ensured. We treat $\tan \beta$ as a free parameter since its interplay with A'_b and A'_τ is central to our present study. The values of various fixed SUSY parameters and the ranges for the ones that are varied are listed in table 1.

Note that we fix ' μ' ' to not too large a value of 500 GeV so that the scenario remains somewhat 'natural'. Given that the contributions to $\Delta_{b,\tau}$ depend significantly on the quantity $\mu + A'_{b,\tau}$, we would thus look out for relatively large $|A'_{b,\tau}|$ to find $\Delta_{b,\tau}$ to be substantially large. Furthermore, we choose a somewhat large value of μ' (1.5 TeV) such that the higgsino-like electroweakinos have masses around $\sim \mu + \mu' = 2$ TeV. Together with M_1 and M_2 set to 2 TeV, these would ensure that the electroweakinos are heavy enough not only to pass the current experimental bounds on them but also to render themselves inaccessible for the ' H ' and the ' A ' states decaying to a pair of them. It may further be noted that the dependence of $\Delta_{b,\tau}$ on μ' is rather weak as long as $\mu + \mu'$ remains smaller than the masses of the gluino and the relevant squark/stau states that are propagating in the loops. This is since μ' enters the expressions for $\Delta_{b,\tau}$ through the integral function $I(a, b, c)$ whose contributions are, as discussed earlier, mostly dictated by the heavier states running in the loops, i.e., the gluino and the squarks/staus, all of which have masses around 3 TeV as indicated in Table 1.

3.1 Variations of $bb\Phi$ and $\tau\tau\Phi$ interaction strengths

The characteristic dependencies of y_b and y_τ and the same for the resulting strengths of the Φbb and $\Phi\tau\tau$ interactions, respectively, where $\Phi \in \{H, A\}$, are discussed in detail in the previous section. In particular, note that the corrections to $y_{b,\tau}$ and the very form of the interactions of these heavy Higgs bosons to a bottom quark or a tau lepton pair in the decoupling regime each lends a separate $\tan\beta$ -dependence to these couplings (see equation 2.14). In addition, in the NHSSM, corrections to $m_{b,\tau}$ ($y_{b,\tau}$) depend on $A'_{b,\tau}$. In this subsection we study these dependencies on $\tan\beta$ and $A'_{b,\tau}$ using the publicly available implementation of the NHSSM model⁴ in the SARAH-v4.14.4 [36, 37]-generated SPheno [38].⁵ Unless otherwise mentioned, all subsequent figures make use of fixed SUSY input parameters of Table 1, conform to $122 \text{ GeV} < m_{h_{\text{SM}}} < 128 \text{ GeV}$ and pass the constraints from HiggsBounds-v5.9.1 [39].

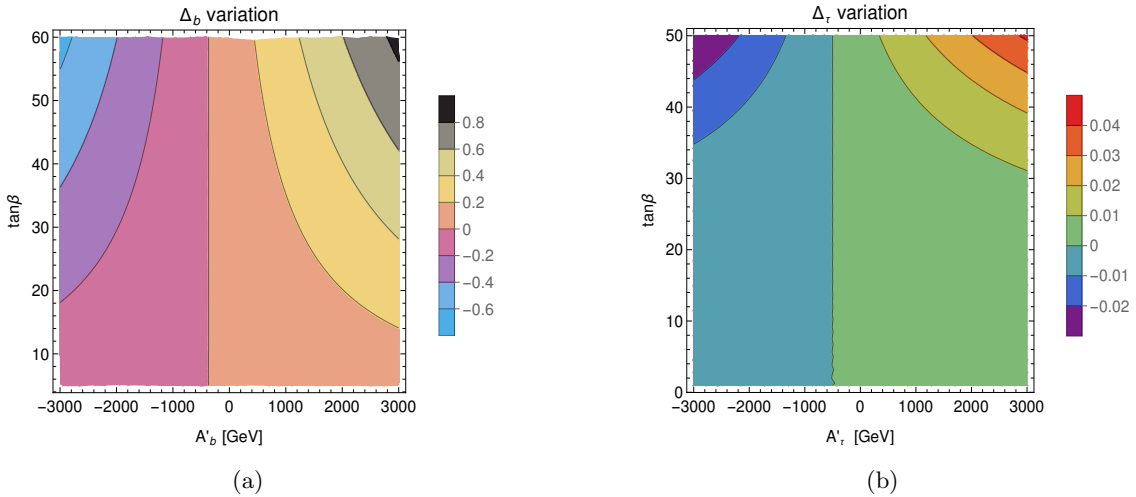


Figure 1. Variations of (a) Δ_b in the $A'_b - \tan\beta$ plane and (b) Δ_τ in the $A'_\tau - \tan\beta$ plane.

First, we discuss the dependence of $y_{b,\tau}$ ($m_{b,\tau}$) on $A'_{b,\tau}$ and $\tan\beta$ arising from radiative corrections to $m_{b,\tau}$. Towards this, a comparative study of the variations of Δ_b and Δ_τ , as functions of A'_b and A'_τ , respectively, and $\tan\beta$, is in order. In figures 1(a) and 1(b) we present such variations of Δ_b and Δ_τ in the $A'_b - \tan\beta$ and $A'_\tau - \tan\beta$ planes, respectively. Visibly, Δ_b could assume much larger values and hence varies over a much larger range when compared to Δ_τ . This is expected since the latter miss out on a gluino-induced, α_s -driven SUSY-QCD correction and also the chargino-induced weak correction (see equation 2.7) while the former benefits from both. Both $|\Delta_b|$ and $|\Delta_\tau|$ grow with growing $\tan\beta$ and with increasing $|A'_b|$ and $|A'_\tau|$, respectively, while their signs broadly follow the signs on the latter two. In this respect, a slight offset about $A'_b(A'_\tau) = 0$ is seen which originates from the term $\mu + A'_b(A'_\tau)$ in equation 2.3 (2.7) and reflects the chosen sign and magnitude of ' μ ' ($= 500 \text{ GeV}$).

As has been noted at the end of section 2.2, a positive (negative) $\Delta_{b,\tau}$ turns the radiatively corrected values of $y_{b,\tau}$ smaller (larger) than their corresponding SM values. In both cases, effects

⁴Some useful patches are kindly provided by the authors of SARAH.

⁵Note that following the convention of SARAH-generated SPheno we absorb y_b in the definition of A'_b , i.e., $A'_b \equiv y_b A'_{b(\text{Soft})}$.

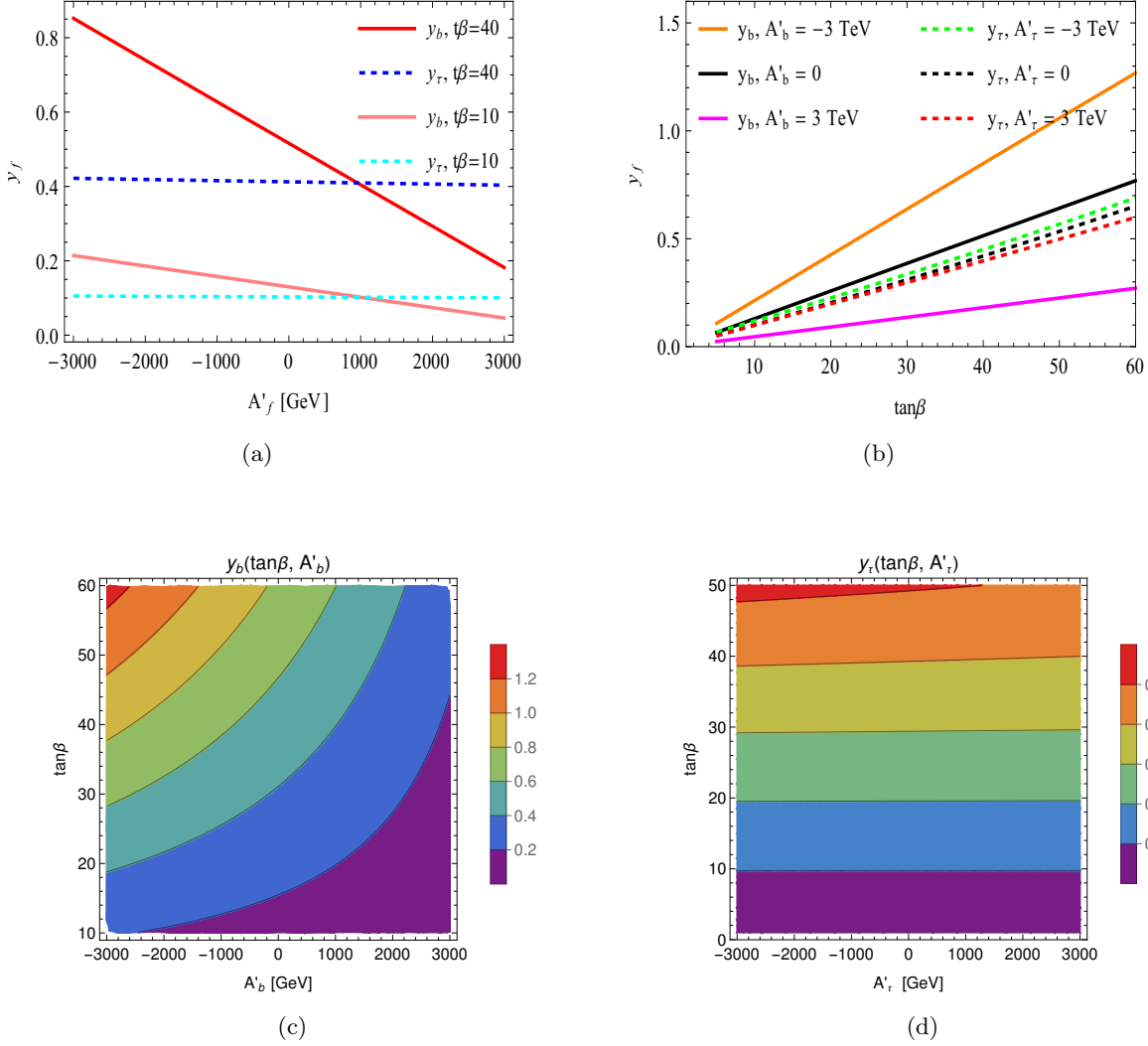


Figure 2. Variations of $y_{f=b,\tau}$ as functions of (a) $A'_{f=b,\tau}$, for two fixed values of $\tan\beta$ (10 and 40) and of (b) $\tan\beta$, for three fixed values of $A'_{f=b,\tau}$ (-3 TeV, 0 and 3 TeV). Variation of y_b (y_τ) in the A'_b (A'_τ) – $\tan\beta$ plane is shown in plot (c) ((d)).

are amplified for larger values of $\tan\beta$. In figure 2(a) we illustrate the variations of $y_{b,\tau}$ and as functions of $A'_{b,\tau}$ for two different values of $\tan\beta$ ($=10$ and 40). The corresponding MSSM values of $y_{b,\tau}$, for any given value of $\tan\beta$, are the ones found at the point of intersection of the particular curve (line) and the line erected vertically at $A'_{b,\tau} = 0$. On the other hand, figure 2(b) shows variations y_b and y_τ as functions of $\tan\beta$ for three different values $A'_{b,\tau}$ ($= -3, 0, 3$ TeV). Again, lines with $A'_{b,\tau} = 0$ (in black) present nothing but the corresponding variations $y_{b,\tau}$ with $\tan\beta$ in the MSSM. These two plots reveal the individual magnitudes of y_b and y_τ as they vary and the ranges of their variations. On both counts, y_b wins over y_τ , hands down, except when A'_b has a large positive value (3 TeV, in the present case). In the latter case, y_b always remains smaller than y_τ for all values of $\tan\beta$ (see the magenta curve) and their difference grows larger with growing $\tan\beta$. A much stronger dependence of y_b on $\tan\beta$ and A'_b , as compared to that of y_τ on $\tan\beta$ and A'_τ can be straightaway traced back to the corresponding dependencies of Δ_b and Δ_τ , respectively, on the

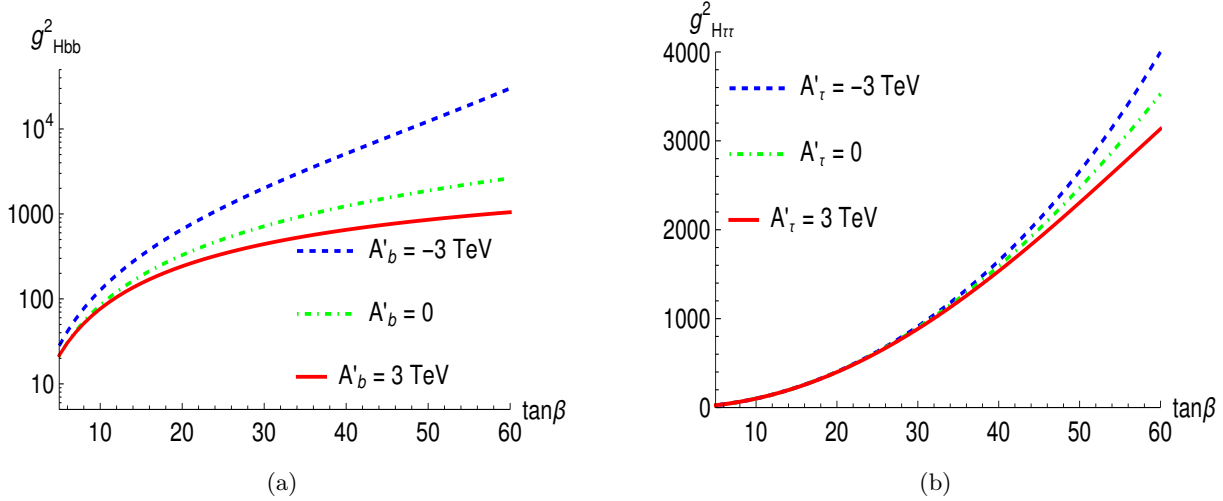


Figure 3. Variations of the squared scaling factors g_{Hbb}^2 (left) and $g_{H\tau\tau}^2$ (right) as functions of $\tan\beta$ and for three fixed values (-3 TeV, 0 and 3 TeV) of A'_b (left) and A'_τ (right).

relevant pairs from these parameters. These two plots further reveal that while y_b is sensitive to both A'_b and $\tan\beta$ (the sensitivity to the former being milder than that to the latter) and assumes larger (smaller) values for large negative (positive) A'_b and large $\tan\beta$, y_τ has an almost exclusive and direct dependence on $\tan\beta$ only. Figure 2(c) (2(d)) captures the same variations but in the plane of $A'_b(A'_\tau) - \tan\beta$.

The resulting variation of the squared value of the reduced coupling strength for $Hbb(\tau\tau)$ interaction, i.e., $g_{Hbb(\tau\tau)}^2$ (see equations 2.14), in the decoupling regime, as a function of $\tan\beta$, is shown in figure 3(a) (3(b)) for $A'_b(A'_\tau) = (-3, 0, 3)$ TeV. Note that while we are compelled to adopt a logarithmic vertical axis for figure 3(a) since g_{Hbb}^2 takes off rather sharply with a growing $\tan\beta$ (thanks to a large negative A'_b and a catalyzing role played by the α_s -dependent contribution to Δ_b), we stick to a linear one in figure 3(b) to illustrate the corresponding variations in $g_{H\tau\tau}^2$ which are much less sensitive to the signs and magnitudes of A'_τ . Curves with $A'_b, A'_\tau = 0$ illustrate such variations in the MSSM-like setups and are shown for reference purposes. As has been noted in section 2.3, for all practical purposes for this work, one can consider $g_{Abb(\tau\tau)}^2 = g_{Hbb(\tau\tau)}^2$. Hence we do not present a separate set of plots for $g_{Abb(\tau\tau)}^2$.

Given the factor $g_{Hbb(\tau\tau)}$ scales the $Hbb(\tau\tau)$ coupling in the SM to its value in the NHSSM, $g_{Hbb(\tau\tau)}^2$ gives us a quick estimate of the factors by which the SM-like values of the associated production cross section $\sigma_{(pp \rightarrow b\bar{b}H/A)}$ and the relevant decay widths $\Gamma(H/A \rightarrow b\bar{b}, \tau\bar{\tau})$ are to be multiplied to find their corresponding values in the NHSSM. In this work we applied such a scaling on the readily available values of $\sigma_{(pp \rightarrow b\bar{b}H/A)}|_{\text{SM}}$ as a function of $m_{H/A}$ (see section 3.3) to find their corresponding values in the NHSSM. On the other hand, although such scalings for $\Gamma(H/A \rightarrow b\bar{b}, \tau\bar{\tau})$ get automatically taken care of in the SARAH-SPheno framework that we use, a quantitative knowledge of the magnitudes of $g_{H/A b\bar{b}(\tau\tau)}^2$ and their nature of variation over the $A'_b(A'_\tau) - \tan\beta$ plane aid a better understanding of the physics interplay in the study of the all important quantity, i.e., $\sigma_{(pp \rightarrow b\bar{b}H/A)} \times \text{BR}[H/A \rightarrow \tau\bar{\tau}]$.

As for how the variations of these couplings affect the LHC studies in context, it may be

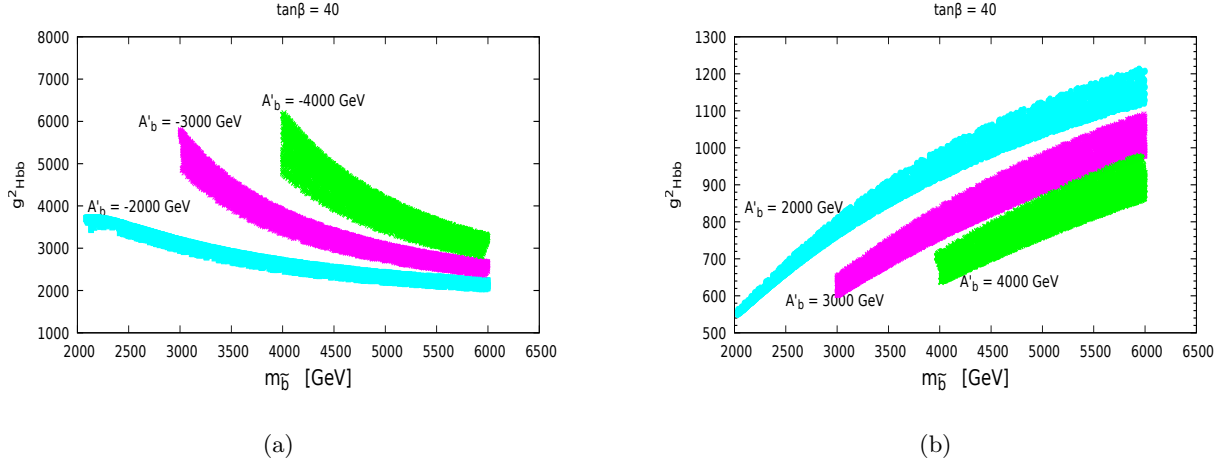


Figure 4. Variations of g_{Hbb}^2 as functions of $m_{\tilde{b}} = m_{\tilde{b}_L} = m_{\tilde{b}_R}$ and for three fixed values of A'_b for each case of (a) $A'_b < 0$ and (b) $A'_b > 0$.

recalled that the exclusion region in the $m_A - \tan\beta$ plane from the searches of neutral heavy Higgs bosons [4–6, 25] is shaped by the variations of the production cross section $\sigma_{(pp \rightarrow b\bar{b}H/A)}$ and the branching fraction $\text{BR}[H/A \rightarrow \tau\bar{\tau}]$ as functions of m_A and $\tan\beta$. As far as NHSSM-specific input parameters are concerned, while the former is controlled by A'_b , the latter are governed collectively by A'_b and A'_τ . Thus, depending upon the combinations of values of A'_b and A'_τ , the reported region of exclusion in the $m_A - \tan\beta$ plane in the MSSM scenario would get altered (either squeezed or extended) when the NHSSM scenario is in context. Quantitatively, however, one can perhaps foresee that the largeness of Δ_b (thanks to the SUSY-QCD correction which is missing in Δ_τ) would control the proceedings except when the input parameters get to be tuned to the contrary. We discuss the decays of the ‘ H ’ and the ‘ A ’ states in section 3.2 and their productions in association with a $b\bar{b}$ pair in section 3.3.

Before we leave this subsection, it would be in order to have a brief discussion on how the other relevant input SUSY parameters, viz., $m_{\tilde{g}}$ and $m_{\tilde{b}_{1,2}}$ could affect the phenomenology. These parameters enter the proceeding effectively through the dominant α_s -dependent term in Δ_b (see equation 2.4). In figure 4 we present the variations of $g_{\Phi bb}^2$ as a function of $m_{\tilde{b}} = m_{\tilde{b}_1} = m_{\tilde{b}_2}$ for three fixed negative (figure 4(a)) and positive (figure 4(b)) values of A'_b . For each chosen value of A'_b we ensure $m_{\tilde{b}} \geq |A'_b|$ such that appearance of CCB minima could be broadly avoided. Bands for different values of A'_b appear due to a varying $m_{\tilde{g}}$ ($3 \text{ TeV} \leq m_{\tilde{g}} \leq 6 \text{ TeV}$). The top (bottom) edge of each band corresponds to the largest (smallest) value of $m_{\tilde{g}}$ used in the scan when $A'_b < 0$. The situation is reversed for $A'_b > 0$. The following observations can be made from the plots in figure 4.

- $g_{\Phi bb}^2$ decreases (increases) with increasing $m_{\tilde{b}}$ for $A'_b < 0$ (> 0).
- $g_{\Phi bb}^2$ increases (decreases) with increasing $m_{\tilde{g}}$ for $A'_b < 0$ (> 0).
- The smallest value (≈ 2000) obtained for $g_{\Phi bb}^2$ with $A'_b < 0$ is larger than the largest value (≈ 1200) found for the same with $A'_b > 0$.

Thus, in our present scheme of analysis, larger values of $g_{\Phi bb}^2$, for $A'_b < 0$, are obtained for a larger $|A'_b| = m_{\bar{b}}$ and a larger $m_{\bar{g}}$. The possible maximum for $g_{\Phi bb}^2$, however, tends to saturate for larger values of $|A'_b| = m_{\bar{b}}$. On the other hand, for $A'_b > 0$, where we ask how small $g_{\Phi bb}^2$ could get, we find that its smallest possible value around 600 (see figure 4(b)) is approached again for $|A'_b| = m_{\bar{b}}$ and for the largest $m_{\bar{g}}$ that we choose. On this occasion, this value of $g_{\Phi bb}^2$ is found to be nearly independent of A'_b . These findings would come in handy when we discuss in section 3.4 how the LHC constraints on the $m_A - \tan \beta$ plane obtained in an MSSM scenario could get altered in the NHSSM scenario.

3.2 Decays of the heavier neutral Higgs bosons

In the decoupling regime, the couplings of the heavier neutral Higgs bosons to gauge bosons ($V \equiv W^\pm, Z$), i.e., $g_{HVV} \propto \cos(\beta - \alpha) \rightarrow 0$. This results in a generic insensitivity in their searches in the modes $H \rightarrow VV$, $A \rightarrow hZ$ etc. Under the circumstances, $H, A \rightarrow t\bar{t}$ would dominate when these Higgs states are sufficiently heavy and $\tan \beta$ is not large. With increasing $\tan \beta$ and hence enhanced $y_{b,\tau}$, the decays $H, A \rightarrow b\bar{b}, \tau\bar{\tau}$ emerge as the only possibilities unless some lighter SUSY states (in particular, the relatively light electroweakinos) are present in the spectrum to which ‘ H ’ and ‘ A ’ could also decay to with moderate branching fractions, a feature that is already present in the MSSM. However, we aim for a simpler setup suited for our purpose where such decays are kinematically forbidden. This is achieved for all $m_{H,A} \leq 3$ TeV by setting $\mu' = 1.5$ TeV, $M_{1,2} = 2$ TeV and $M_3 = 3$ TeV (see table 1).

In the NHSSM, decays of H/A to final states involving b, τ get further affected if $A'_b, A'_\tau \neq 0$ since these control the magnitudes of y_b and y_τ , respectively. As expected, this could well modify the experimental sensitivities of searches of heavier Higgs bosons in these final states. Consequently, the exclusion region in the $m_A - \tan \beta$ plane as obtained for the MSSM scenario would get altered for the NHSSM case. Here, it is important to point out that although the decays of heavier Higgs bosons to bottom quarks dominate at larger $\tan \beta$ (and large negative A'_b), final states involving b -jets are prone to large jetty backgrounds from the SM. Hence searches for the heavy Higgs states at the LHC are best carried out in the subdominant modes involving the τ 's. Note, however, that while y_b (and not y_τ) controls $\sigma(pp \rightarrow b\bar{b}H/A)$, $\text{BR}[H/A \rightarrow \tau\bar{\tau}]$ are controlled by both y_b and y_τ . The highest sensitivity to the $\tau\bar{\tau}$ final state is thus attained when the right balance in the magnitudes of y_b and y_τ is struck over the NHSSM parameter space.

Given that the magnitudes and the patterns of variations of branching fractions to $b\bar{b}$ and $\tau\bar{\tau}$ of the ‘ H ’ and ‘ A ’ states are expected (and found) to be very similar, a common representative illustration of these variations for the two states would suffice. In addition, the complementarity of $\text{BR}[H/A \rightarrow b\bar{b}]$ and $\text{BR}[H/A \rightarrow \tau\bar{\tau}]$ allows us to discuss the proceedings in terms of any one of these quantities. The obvious choice is then $\text{BR}[H/A \rightarrow \tau\bar{\tau}]$ since the concerned experimental analyses consider the decays $H/A \rightarrow \tau\bar{\tau}$. It may further be noted that $\text{BR}[H/A \rightarrow \tau\bar{\tau}]$ depends not only on $\tan \beta$ and A'_τ but also on A'_b . This is since A'_b influences the partial decay width for $H/A \rightarrow b\bar{b}$ which, in turn, affects $\text{BR}[H/A \rightarrow \tau\bar{\tau}]$ by altering the total decay width of H/A that enters the computation of the branching fractions.

In figure 5 we present the variations of $\text{BR}[H/A \rightarrow \tau\bar{\tau}]$ in the $A'_b - A'_\tau$ plane for $\tan \beta = 10$ (figure 5(a)) and $\tan \beta = 40$ (figure 5(b)) when $m_{H,A}$ are set at a value of 2.5 TeV. It is seen that, irrespective of the value of $\tan \beta$, the dependence of $\text{BR}[H/A \rightarrow \tau\bar{\tau}]$ on A'_τ is only rather mild.

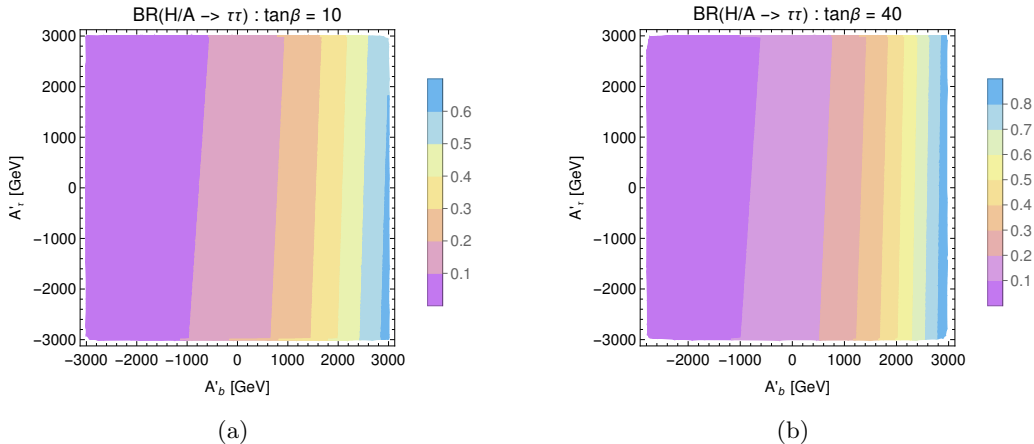


Figure 5. Variations of $\text{BR}[H/A \rightarrow \tau\bar{\tau}]$ in the $A'_b - A'_\tau$ plane for (a) $\tan\beta = 10$ and (b) $\tan\beta = 40$ and for $m_{H,A} = 2.5$ TeV.

Thus, it is A'_b which almost single-handedly dictates $\text{BR}[H/A \rightarrow \tau\bar{\tau}]$. As discussed in section 2.3, this can be traced back to the smallness of Δ_τ when compared to Δ_b as the former lacks the gluonic (strong) contribution. It may further be noted how rapidly $\text{BR}[H/A \rightarrow \tau\bar{\tau}]$ drops as A'_b decreases from its large positive value. Hence, for any given $\tan\beta$, the only situation when decays to $\tau\bar{\tau}$ could be comparable to (or may even dominate) those to $b\bar{b}$ is when A'_b has a large enough positive value thus rendering the couplings $H/Ab\bar{b}$ much smaller compared to those for $H/A\tau\bar{\tau}$. As can be found from figure 5, under such a circumstance, $\text{BR}[H, A \rightarrow \tau\bar{\tau}]$ could reach $\sim 90\%$ when $\tan\beta$ is large while $\text{BR}[H, A \rightarrow \tau\bar{\tau}]$ dropping to a mere $\sim 10\%$.

It is important here to note that, for any given integrated luminosity, for the LHC experiments to be sensitive to searches for the H/A states in the mode $pp \rightarrow b\bar{b}H, A$ followed by $H, A \rightarrow \tau\bar{\tau}$, the product $\sigma(pp \rightarrow b\bar{b}H/A) \times \text{BR}[H/A \rightarrow \tau\bar{\tau}]$ has to be optimally large. With A'_b effectively controlling both these quantities but that being in a contrasting manner, only an optimal value of A'_b would maximize the said product, for any given set of other input parameters.

3.3 Production of heavier neutral Higgs bosons (H, A) with a bottom quark pair

Predicting the production cross section of a Higgs boson in association with a pair of b -quarks at hadron colliders involves theoretical subtleties. m_b being small yet may not be ignored, there are two competing approaches to calculate the hard, parton level cross section: the so-called 4-flavor scheme (4FS) and the 5-flavor scheme (5FS). These entail different perturbation expansions of the same physical observables, i.e., $pp \rightarrow \text{Higgs} + jets$, which start contributing at different perturbation orders in α_s . Their close agreement is then expected only at sufficiently high orders [35].

In the 4FS, the b -quark is taken to be massive. Hence the proton (or the antiproton) parton distribution contains gluons and the four light (\sim massless) flavor quarks, u, d, s, c and the corresponding antiquarks. The relevant parton level processes at the LHC, at the lowest order (LO) in perturbation theory, are then driven by gluon-fusion and quark-antiquark annihilation, i.e.,

$$gg, q\bar{q} \rightarrow b\bar{b} H/A. \quad (3.1)$$

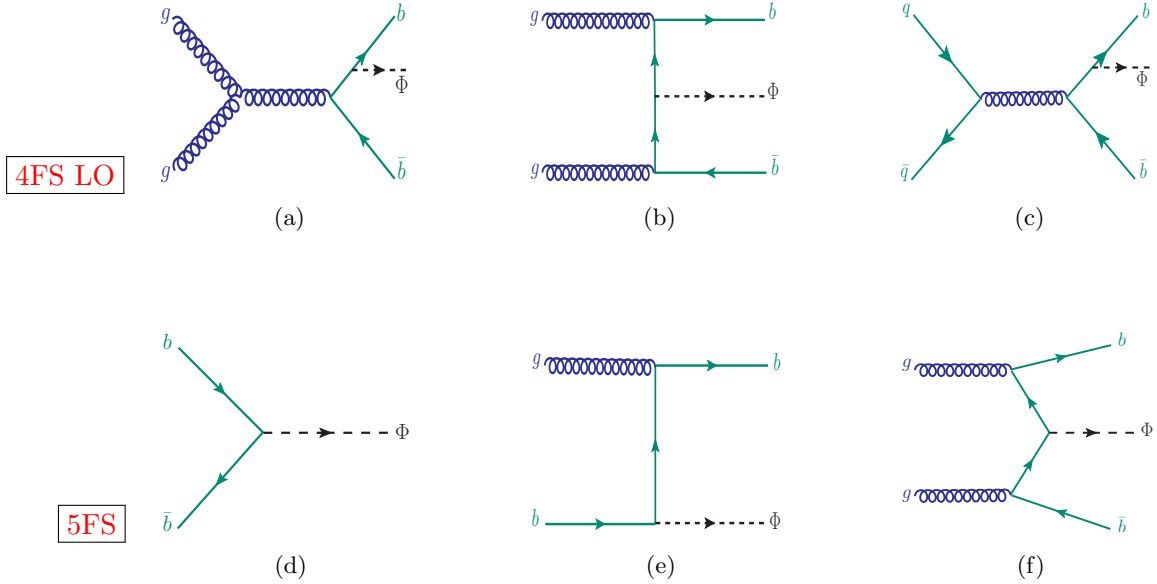


Figure 6. Representative 4FS LO Feynman diagrams contributing to exclusive $b\bar{b}\Phi$ ($\Phi = h, H, A$) production in the 4FS (top panel) and the ones for the corresponding inclusive process at LO (left), NLO (middle) and NNLO (right) in the 5FS (bottom panel). See text for details.

A generic, representative set of Feynman diagrams for this (4FS LO) category is shown in the upper panel of figure 6. At the LHC energies, the LO cross section is largely dominated by the gluon fusion process. Note that the t -channel gluon-fusion process in figure 6(b) leads to large logarithms $\sim \ln(\mu_F^2/m_b^2)$ on integrating over the phase space of the final state b -quarks; $\mu_F \sim m_{\Phi \in H, A}$ being the so-called factorization scale. In the computation of an inclusive cross section of the sort, such large logarithms (involving finite m_b) are effectively resummed to all orders via the introduction of the b -quark parton distribution function (PDF) [40] in the proton with $m_b \rightarrow 0$ when final state b -quarks emerge with small p_T . This is the 5FS. A representative set of Feynman diagrams in this scheme for the inclusive process in reference is shown in the lower panel of figure 6.

The fully inclusive cross section in the 5FS would then be dominated by the LO process $b\bar{b} \rightarrow \Phi$ [41] in figure 6(d) and exceeds the corresponding 4FS LO estimates. This can be understood by noting that the dominant 4FS LO process (the t -channel one of figure 6(b)) appears only at the next-to-next-to-leading order (NNLO)-QCD in the 5FS, as shown in 6(f). It is further observed that the 4FS (5FS) approach is better suited in the asymptotic limit of small (large) Higgs boson masses when the mass of the bottom quark cannot (can) be neglected as is the defining characteristic of the scheme [42].

Experiments studying $pp \rightarrow b\bar{b}\Phi$ necessarily have to tag b -jet(s). An exclusive search like this requires a minimum $p_T^{(b)}$ which ensures that the tagged b -jets do not have their origins in the b -quark PDF. Hence one may rely exclusively on the 4FS for the LO rates. This further guarantees that the Higgs boson to have been radiated off one such final state b -quark produced in the hard scattering thus probing y_b directly.

Eventually, bounds derived from the experiments on $\sigma_{(pp \rightarrow b\bar{b}H/A)} \times \text{BR}[H/A \rightarrow \tau\bar{\tau}]$, and on the $m_A - \tan\beta$ plane thereon [43–45], refer to the inclusive (total) cross sections. In either of these

two schemes, more precise estimates of these cross sections, which are stable against variations in the unphysical factorization/renormalization (μ_R) scales, can only be found by including higher order corrections.

Given that the computation of the higher-order corrections is simpler in the 5FS (since $m_b \rightarrow 0$ and the LO process is a resonant one), cross sections up to NNLO (in α_s) are known there for long [46–48]. In contrast, rates only up to next-to-leading order (NLO) are available in the 4FS [2, 49, 50].⁶ At these available orders, the cross sections obtained in the two schemes tend to show improved agreements along with a much milder dependence on μ_F and μ_R . In spite of this, 4FS NLO results are unable to capture logarithmic terms beyond the first few while the 5FS NNLO ones fail to do so for the so-called power-suppressed terms [2].⁷

Capturing the best from the two different kinematic regimes requires a systematic combination of these contributions [42, 53–58]. Here, we adopt an improved approach called FNOLL-B [59–62] as also done by a recent ATLAS analysis [45]. This approach combines the 4FS-NLO accuracy with the accuracy of NNLO leading-log (NNLL) for the resummed collinear logarithms of the 5FS.⁸ Towards this, we follow the recommendations of references [64, 65]. Hence we use the cross sections for $pp \rightarrow b\bar{b}H$ quoted there as a function of m_H [60, 61] where the Hbb coupling is SM-like and $\mu_{FR} = \mu_F = \mu_R = (m_H + 2m_b)/4$.⁹ These rates are indicated to be cross-checked against the FNOLL-B matched results of reference [62].

We obtain $\sigma(pp \rightarrow b\bar{b}H/A)|_{\text{NHSSM}}$ by an appropriate rescaling of y_b [71–73], i.e., by multiplying $\sigma(pp \rightarrow b\bar{b}h_{\text{SM}})$ by the square of the factors $g_{b\bar{b}H/A}$ of equations 2.12 that are now computed for the NHSSM. It should be noted that, over the broad range of $m_{H/A}$ we consider, their mass-differences are found to be smaller than the experimental resolution (except when $m_A \leq 400$ GeV). Hence these states are treated as mass-degenerate [45]. Thus, for any given mass $m_{H/A}$, their contributions are just added up.

In figure 7 we present the variations of the combined cross sections for $pp \rightarrow b\bar{b}H, A$ at the 13 TeV LHC in the m_A - $\tan\beta$ plane for (a) $A'_b = 3$ TeV, (b) $A'_b = 0$ (the MSSM-like case) and (c) $A'_b = -3$ TeV. As can be seen from these plots, for large $\tan\beta$ and larger m_A , the cross sections with $A'_b = -3$ TeV could be up to a couple of orders larger in magnitude than that when $A'_b = 3$ TeV. The plot in the middle ($A'_b = 0$) serves as an MSSM-reference for the purpose in which, for any given values of m_A and $\tan\beta$, one finds intermediate values of cross sections when compared to the former two cases. The patterns of variations of the cross section are intimately related to the same for the respective variation of y_b (see figure 2), or for that matter, of $g_{b\bar{b}H/A}^2$ (see figure 3) in the same parameter-plane and also shape the projected exclusions obtained in the NHSSM scenario in section 3.4.

⁶This calculation is recently improved to contain NLO-electroweak corrections [3].

⁷Of recent, next-to-next-to-next-to leading order (N³LO) [51] and N³-leading log (N³LL) [52] estimates in the 5FS have become available and are found to agree even more closely with the NLO-QCD one in the 4FS.

⁸Recently, an even more accurate prediction of the inclusive production cross section by matching 4FS-NLO results with those from the 5FS N³LO ones has been made [63].

⁹Note that μ_{FR} is much smaller than m_H itself and is known to lead to reasonable agreements between 4FS and 5FS estimates already at LO and NLO [48, 66, 67] with improved perturbative convergence [60, 66, 68–70].

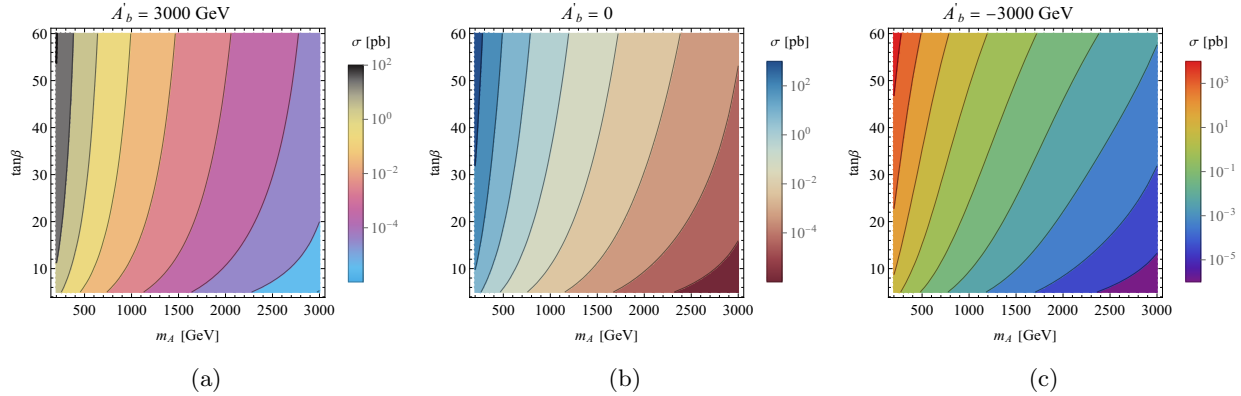


Figure 7. Variations of cross sections $\sigma_{(pp \rightarrow b\bar{b}H + b\bar{b}A)}$ (in pb) at the 13 TeV LHC in the $m_A - \tan\beta$ plane for (a) $A'_b = 3$ TeV, (b) $A'_b = 0$ and (c) $A'_b = -3$ TeV.

3.4 Constraining $m_A - \tan\beta$ plane: NHSSM vis-a-vis LHC exclusion (in the MSSM)

As pointed out in section 3.1, the sensitivity of a search for a heavy Higgs boson via its associated production with a b -quark pair, at the LHC, broadly depends on the quantity $\sigma(pp \rightarrow b\bar{b}H/A)$ times the branching fraction of H/A into an optimally sensitive mode which happens to be the $\tau\bar{\tau}$ mode. Recent LHC analyses [43–45] have put constraints (at 95% confidence level (CL)) on the maximum allowed values of the product $\sigma(pp \rightarrow b\bar{b}\Phi) \times \text{BR}[\Phi \rightarrow \tau\bar{\tau}]$ as a function of m_Φ , in a model-independent way. These are then translated into a model-dependent (MSSM) exclusion contour (again at 95% CL) in the plane of m_A and $\tan\beta$, the sole unknown parameters of the theoretical setup in reference on which the observable quantity under consideration depends. Given that both $\sigma(pp \rightarrow b\bar{b}H/A)$ and $\text{BR}[H/A \rightarrow \tau\bar{\tau}]$ crucially depend on an NHSSM-specific parameter like A'_b , in addition to their usual (MSSM-type) dependencies on m_A and $\tan\beta$, the existing domain of exclusion in the $m_A - \tan\beta$ plane for the MSSM-like limit (i.e., $A'_b = 0$) is bound to get altered in the NHSSM as A'_b varies. We work out such exclusion contours in the NHSSM scenario and contrast those with the one from a recent ATLAS analysis [45] that provides the strongest exclusion till date on the $m_A - \tan\beta$ plane.

In figure 8(a) we study the variations of $\sigma \times \text{BR}$ as functions of $m_{H/A}$ for two discrete values of each of $\tan\beta$ (10 and 40) and A'_b (-3 TeV and 3 TeV)¹⁰ and contrast those with its observed upper limits (at 95% confidence limit (CL)) as reported by the ATLAS collaboration (in figure 2(b) of reference [45]) and represented by the lower/left edge of the grey region in figure 8(a). The sections of the blue and the red curves falling within the grey region indicate the values of $m_{H/A}$ that are ruled out in the NHSSM for different combinations of $\tan\beta$ and A'_b . As is expected, the largest (smallest) of the values of $m_{H/A}$ is ruled out with the dashed-blue (solid-red) curves for which $\tan\beta$ is large (small) and A'_b is negative (positive).

¹⁰As mentioned earlier, ‘ H ’ and ‘ A ’ states could practically be considered mass-degenerate over the considered range of their masses. Hence, for the purpose in hand, for any given mass $m_A = m_H$, their production cross sections are added up and then multiplied by a branching fraction to $\tau\bar{\tau}$ which happens to be essentially the same for the two Higgs states, in particular, in the scenario under consideration where their decays to only the SM states are kinematically allowed.

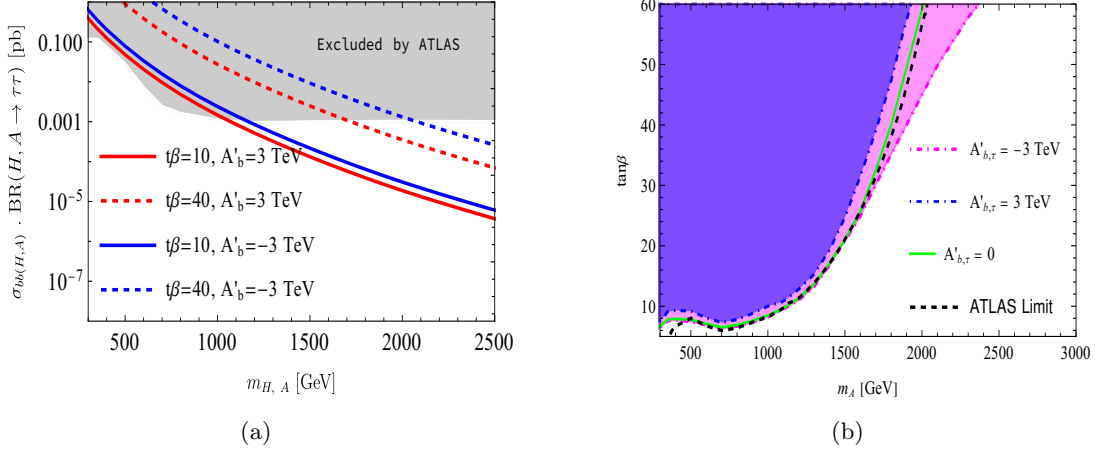


Figure 8. (a) Varying $\sigma \times \text{BR}$ for different values of A'_b and $\tan \beta$, as a function of $m_{\Phi=H,A}$, shown against its observed upper limits at 95% CL as reported in figure 2(b) of reference [45] and defined by the lower/left edge of the grey region and (b) the results of recasting the observed ATLAS upper limits on $\sigma \times \text{BR}$ in figure 8(a) on the $m_A - \tan \beta$ plane for various representative values of A'_b . In figures 8(a) and 8(b), curves representing the reinforced (relaxed) bounds are obtained using the combination $A'_{b,\tau} = -(+)$ 3 TeV.

The same analysis for the NHSSM is then ported to delineate the altered excluded regions in the $m_A - \tan \beta$ plane vis-a-vis the one presented by the mentioned ATLAS experiment [45] for a generic MSSM scenario called the M_h^{125} scenario [74] whose defining features are all preserved in the NHSSM scenario we adopt in this work. While contrasting our findings with the experimental one, we limit ourselves to the associated $b\bar{b}H, A$ productions whereas the experiment considers the gluon fusion process as well for the production of these Higgs states. It may, however, be noted that at larger values of $\tan \beta$, where we find the NHSSM effects to be somewhat prominent, $pp \rightarrow b\bar{b}H, A$ play the dominant role [6]. Hence, given the scope of the present work, our approach suffices. The closely overlapping dashed contours in green and black in figure 8(b) represent our derivation of the exclusion region with $A'_b = 0$ (the MSSM limit for the concerned sector) and the same obtained for the M_h^{125} -MSSM scenario by the ATLAS experiment (at 95% CL; in figure 2(c) of reference [45]), respectively. In NHSSM scenarios with $A'_b \neq 0$, one finds a slightly relaxed exclusion (to the edge of the purple region) for $A'_b > 0$ and for all values of $\tan \beta$ (when compared to the same obtained for the M_h^{125} -MSSM scenario) and a reinforced one (to the edge of the pink region) for $A'_b < 0$ only when $\tan \beta$ is on the larger side (≥ 30). Note that for the curves showing maximal deviations in $\sigma \times \text{BR}$ in figure 8(a) and hence maximal alterations in the exclusion limits in figure 8(b), with respect to the $A'_b = 0$ case, are obtained with combinations of $A'_{b,\tau}$ with maximal values we use for them (i.e., $|A'_{b,\tau}| = 3$ TeV) and setting $\text{sign}(A'_{b,\tau})$ to be the same as that on A'_b which broadly controls the nature of such alterations. We have checked that all these findings also agree closely with the exclusion obtained using HiggsBounds-v5.9.1 which now incorporates the pertinent ATLAS analysis in reference [45].

The nature of the modified exclusion contours could be broadly reconciled by referring to the same for the variations of $\text{BR}(H/A \rightarrow \tau\bar{\tau})$ and the cross section $\sigma_{(pp \rightarrow b\bar{b}H/A)}$ as illustrated in figures 5 and 7, respectively. Of particular interest is the asymmetric nature of the possible relaxations and

reinforcements in the exclusions in the NHSSM scenario that are obtained using somewhat large (extremal) values of A'_b and $\tan\beta$, when compared to the exclusions obtained for the MSSM case. Note from figure 5 that $\text{BR}(H/A \rightarrow \tau\bar{\tau})$ more or less saturates as A'_b and $\tan\beta$ approach large values irrespective of the sign on A'_b . However, while for large, positive A'_b , $\text{BR}(H/A \rightarrow \tau\bar{\tau})$ reaches a plateau at a larger value compared to the MSSM case, the reverse is true for large, negative A'_b . On top of that, from figures 7(a) and 7(b) (the MSSM case) one can find that the cross sections in these two scenarios for any given $\tan\beta$ and A'_b are not too different. Hence the product $\sigma \times \text{BR}$ remains nearly as sensitive to the experiment as for the MSSM case. This is behind a minor relaxation in the exclusions even when the setup favors a maximum. On the other hand, it can be gleaned from figure 7(c) that for large, negative A'_b , the difference in the cross sections $\sigma_{(pp \rightarrow b\bar{b}H/A)}$ with that from the MSSM scenario quickly grows for growing m_A and $\tan\beta$. Though $\text{BR}(H/A \rightarrow \tau\bar{\tau})$ tends to saturate at a value lower than that in the MSSM case, it is entirely because of the rapid growth in the cross section with $\tan\beta$ that drives the sensitivity to the experiment and hence an extended exclusion of the $m_A - \tan\beta$ space for large, negative A'_b . At a more fundamental level, these features are perhaps best understood in terms of the variations of $y_{b,\tau}(\tan\beta, A'_b)$ as shown in figure 2(b) and then, of $g_{Hbb}^2(\tan\beta, A'_b)$ as shown in figures 3(a) and 3(b).

In this context, it is noteworthy that the extents of relaxation and reinforcement of exclusions that are presented in figure 8(b) both refer to NHSSM scenarios that are cut out for yielding such alterations to be nearly maximal. The only way such modifications could get somewhat pronounced is by setting $m_{\tilde{g}}$ at a value higher than what we have used, i.e., 3 TeV (in fact, this is the smallest value from the range we have used to draw the plots in figure 4. On these plots, at $|A'_b| = m_{\tilde{b}}$, the widths of the bands are the largest and we are referring to the lowest (highest) points from these bands at $|A'_b| = m_{\tilde{b}}$ for $A'_b < 0 (> 0)$.

4 Conclusions

In this work, we have discussed in detail the nature of the dependencies of each of the bottom and the tau Yukawa couplings simultaneously on the NHSSM-specific trilinear soft parameters A'_b and A'_τ , respectively, and on $\tan\beta$. The MSSM higgsino mass parameter is held at not too large a value (500 GeV) thus aiding the scenario to remain somewhat ‘natural’. We have further undertaken a thorough investigation on how these could affect, in the NHSSM scenario, the production cross sections of the heavy neutral Higgs bosons (H and A) in association with a b -quark pair and their branching fractions to $\tau\bar{\tau}$, the two key ingredients that dictate their reach at the current and future runs of the LHC. These are demonstrated in terms of altered (relaxed or extended) exclusion regions in the customary $m_A - \tan\beta$ plane and contrasted with the latest such constraint from the LHC for an MSSM scenario, for some representative values of A'_b . The role of A'_τ is found to be rather limited while the same of the masses of the sbottom and the gluino can be moderate.

A general finding is that such deviations are maximal when both $\tan\beta$ and the magnitude of A'_b are large. For an example, for $\tan\beta = 60$, while a maximum relaxation of ≈ 100 GeV in m_A is observed in the NHSSM scenario for a large positive A'_b ($= 3$ TeV) when in the MSSM it is excluded up to 2 TeV, a strengthening of the exclusion by about 350 GeV with respect to the latter occurs for a large negative A'_b ($= -3$ TeV). For smaller values of $\tan\beta$, the role of A'_b is set to diminish since, in that regime, A'_b affects $\sigma(pp \rightarrow b\bar{b}H, A)$ and $\text{BR}[H, A \rightarrow \tau\bar{\tau}]$ in a complementary way such that the all-important quantity $\sigma \times \text{BR}$ ceases to be sensitive to a variation in A'_b . Thus, for smaller

values of $\tan\beta$, the exclusion contour in the $m_A - \tan\beta$ plane in the NHSSM scenario does not deviate much from the reported (MSSM) one. Overall, unless for a rather large value of $\tan\beta$, the relevant NHSSM parameters tend to conspire such that the LHC sensitivity of the scenario does not differ much from the MSSM case. As far as the exclusion of the $m_A - \tan\beta$ parameter plane is concerned, this pattern is expected to be broadly preserved at the upcoming runs of the LHC.

Acknowledgements

AKS thanks the Department of Physics, SGTB Khalsa College, University of Delhi and the SERB sponsored Multi Institutional Project titled ‘‘Probing New Physics Interactions’’ (CRG/2018/004889) running there under which the major part of the work has been carried out. The authors also like to thank Mark Goodsell for many useful discussions on various aspects of the implementation of the NHSSM scenario in **SPheno** via **SARAH**. They also thank Arnaud Ferrari from the ATLAS Collaboration, Rikkert Frederix, Jean-Loic Kneur, Davide Napoletano, Werner Porod and V. Ravindran for very helpful exchanges.

References

- [1] G. Aad *et al.* [ATLAS], Phys. Rev. D **101** (2020) no.1, 012002 doi:10.1103/PhysRevD.101.012002 [arXiv:1909.02845 [hep-ex]].
- [2] M. Wiesemann, R. Frederix, S. Frixione, V. Hirschi, F. Maltoni and P. Torrielli, JHEP **02** (2015), 132 doi:10.1007/JHEP02(2015)132 [arXiv:1409.5301 [hep-ph]].
- [3] D. Pagani, H. S. Shao and M. Zaro, JHEP **11** (2020), 036 doi:10.1007/JHEP11(2020)036 [arXiv:2005.10277 [hep-ph]].
- [4] A. M. Sirunyan *et al.* [CMS], JHEP **09** (2018), 007 doi:10.1007/JHEP09(2018)007 [arXiv:1803.06553 [hep-ex]].
- [5] G. Aad *et al.* [ATLAS], Phys. Rev. Lett. **125** (2020) no.5, 051801 doi:10.1103/PhysRevLett.125.051801 [arXiv:2002.12223 [hep-ex]].
- [6] M. Aaboud *et al.* [ATLAS], JHEP **01** (2018), 055 doi:10.1007/JHEP01(2018)055 [arXiv:1709.07242 [hep-ex]].
- [7] L. Girardello and M. T. Grisaru, Nucl. Phys. B **194** (1982), 65 doi:10.1016/0550-3213(82)90512-0
- [8] S. P. Martin, Phys. Rev. D **61** (2000), 035004 doi:10.1103/PhysRevD.61.035004 [arXiv:hep-ph/9907550 [hep-ph]].
- [9] G. G. Ross, K. Schmidt-Hoberg and F. Staub, Phys. Lett. B **759** (2016) 110 doi:10.1016/j.physletb.2016.05.053 [arXiv:1603.09347 [hep-ph]].
- [10] G. G. Ross, K. Schmidt-Hoberg and F. Staub, JHEP **1703** (2017) 021 doi:10.1007/JHEP03(2017)021 [arXiv:1701.03480 [hep-ph]].
- [11] U. Chattopadhyay, D. Das and S. Mukherjee, JHEP **01** (2018), 158 doi:10.1007/JHEP01(2018)158 [arXiv:1710.10120 [hep-ph]].
- [12] S. Chakraborty and T. S. Roy, Phys. Rev. D **100**, no.3, 035020 (2019) doi:10.1103/PhysRevD.100.035020 [arXiv:1904.10144 [hep-ph]].
- [13] H. E. Haber and J. D. Mason, Phys. Rev. D **77** (2008), 115011 doi:10.1103/PhysRevD.77.115011 [arXiv:0711.2890 [hep-ph]].

- [14] J. Bagger and E. Poppitz, Phys. Rev. Lett. **71** (1993), 2380-2382 doi:10.1103/PhysRevLett.71.2380 [arXiv:hep-ph/9307317 [hep-ph]].
- [15] U. Ellwanger, Phys. Lett. B **133** (1983), 187-191 doi:10.1016/0370-2693(83)90557-9
- [16] I. Jack and D. R. T. Jones, Phys. Lett. B **457** (1999), 101-108 doi:10.1016/S0370-2693(99)00530-4 [arXiv:hep-ph/9903365 [hep-ph]].
- [17] U. Chattopadhyay and A. Dey, JHEP **10** (2016), 027 doi:10.1007/JHEP10(2016)027 [arXiv:1604.06367 [hep-ph]].
- [18] U. Chattopadhyay, A. Datta, S. Mukherjee and A. K. Swain, JHEP **10** (2018), 202 doi:10.1007/JHEP10(2018)202 [arXiv:1809.05438 [hep-ph]].
- [19] L. J. Hall, R. Rattazzi and U. Sarid, Phys. Rev. D **50** (1994), 7048-7065 doi:10.1103/PhysRevD.50.7048 [arXiv:hep-ph/9306309 [hep-ph]].
- [20] R. Hempfling, Phys. Rev. D **49** (1994), 6168-6172 doi:10.1103/PhysRevD.49.6168
- [21] M. Carena, M. Olechowski, S. Pokorski and C. E. M. Wagner, Nucl. Phys. B **426** (1994), 269-300 doi:10.1016/0550-3213(94)90313-1 [arXiv:hep-ph/9402253 [hep-ph]].
- [22] D. M. Pierce, J. A. Bagger, K. T. Matchev and R. j. Zhang, Nucl. Phys. B **491** (1997), 3-67 doi:10.1016/S0550-3213(96)00683-9 [arXiv:hep-ph/9606211 [hep-ph]].
- [23] H. E. Logan, Nucl. Phys. B Proc. Suppl. **101** (2001), 279-288 doi:10.1016/S0920-5632(01)01512-2 [arXiv:hep-ph/0102029 [hep-ph]].
- [24] S. Antusch and M. Spinrath, Phys. Rev. D **78** (2008), 075020 doi:10.1103/PhysRevD.78.075020 [arXiv:0804.0717 [hep-ph]].
- [25] M. Aaboud *et al.* [ATLAS], JHEP **09** (2018), 139 doi:10.1007/JHEP09(2018)139 [arXiv:1807.07915 [hep-ex]].
- [26] G. Aad *et al.* [ATLAS], JHEP **06** (2021), 145 doi:10.1007/JHEP06(2021)145 [arXiv:2102.10076 [hep-ex]].
- [27] G. Aad *et al.* [ATLAS], JHEP **05** (2021), 093 doi:10.1007/JHEP05(2021)093 [arXiv:2101.12527 [hep-ex]].
- [28] A. Dedes and S. Moretti, Phys. Rev. D **60** (1999), 015007 doi:10.1103/PhysRevD.60.015007 [arXiv:hep-ph/9812328 [hep-ph]].
- [29] J. Beuria and A. Dey, JHEP **10** (2017), 154 doi:10.1007/JHEP10(2017)154 [arXiv:1708.08361 [hep-ph]].
- [30] A. Crivellin, Phys. Rev. D **83** (2011), 056001 doi:10.1103/PhysRevD.83.056001 [arXiv:1012.4840 [hep-ph]].
- [31] A. Crivellin, L. Hofer and J. Rosiek, JHEP **07** (2011), 017 doi:10.1007/JHEP07(2011)017 [arXiv:1103.4272 [hep-ph]].
- [32] A. Crivellin and C. Greub, Phys. Rev. D **87** (2013), 015013 [erratum: Phys. Rev. D **87** (2013), 079901] doi:10.1103/PhysRevD.87.015013 [arXiv:1210.7453 [hep-ph]].
- [33] A. Djouadi, Phys. Rept. **459** (2008), 1-241 doi:10.1016/j.physrep.2007.10.005 [arXiv:hep-ph/0503173 [hep-ph]].
- [34] I. F. Ginzburg, M. Krawczyk and P. Osland, [arXiv:hep-ph/0211371 [hep-ph]].
- [35] S. Dawson, C. B. Jackson, L. Reina and D. Wackerroth, Mod. Phys. Lett. A **21** (2006), 89-110 doi:10.1142/S0217732306019256 [arXiv:hep-ph/0508293 [hep-ph]].

- [36] F. Staub, *Comput. Phys. Commun.* **185** (2014), 1773-1790 doi:10.1016/j.cpc.2014.02.018 [arXiv:1309.7223 [hep-ph]].
- [37] F. Staub, *Adv. High Energy Phys.* **2015** (2015), 840780 doi:10.1155/2015/840780 [arXiv:1503.04200 [hep-ph]].
- [38] W. Porod and F. Staub, *Comput. Phys. Commun.* **183** (2012), 2458-2469 doi:10.1016/j.cpc.2012.05.021 [arXiv:1104.1573 [hep-ph]].
- [39] P. Bechtle, D. Dercks, S. Heinemeyer, T. Klingl, T. Stefaniak, G. Weiglein and J. Wittbrodt, *Eur. Phys. J. C* **80** (2020) no.12, 1211 doi:10.1140/epjc/s10052-020-08557-9 [arXiv:2006.06007 [hep-ph]].
- [40] R. M. Barnett, H. E. Haber and D. E. Soper, *Nucl. Phys. B* **306** (1988), 697-745 doi:10.1016/0550-3213(88)90440-3
- [41] D. A. Dicus and S. Willenbrock, *Phys. Rev. D* **39** (1989), 751 doi:10.1103/PhysRevD.39.751
- [42] R. Harlander, M. Kramer and M. Schumacher, [arXiv:1112.3478 [hep-ph]].
- [43] M. Aaboud *et al.* [ATLAS], *JHEP* **01** (2018), 055 doi:10.1007/JHEP01(2018)055 [arXiv:1709.07242 [hep-ex]].
- [44] A. M. Sirunyan *et al.* [CMS], *JHEP* **09** (2018), 007 doi:10.1007/JHEP09(2018)007 [arXiv:1803.06553 [hep-ex]].
- [45] G. Aad *et al.* [ATLAS], *Phys. Rev. Lett.* **125** (2020) no.5, 051801 doi:10.1103/PhysRevLett.125.051801 [arXiv:2002.12223 [hep-ex]].
- [46] D. Dicus, T. Stelzer, Z. Sullivan and S. Willenbrock, *Phys. Rev. D* **59** (1999), 094016 doi:10.1103/PhysRevD.59.094016 [arXiv:hep-ph/9811492 [hep-ph]].
- [47] C. Balazs, H. J. He and C. P. Yuan, *Phys. Rev. D* **60** (1999), 114001 doi:10.1103/PhysRevD.60.114001 [arXiv:hep-ph/9812263 [hep-ph]].
- [48] R. V. Harlander and W. B. Kilgore, *Phys. Rev. D* **68** (2003), 013001 doi:10.1103/PhysRevD.68.013001 [arXiv:hep-ph/0304035 [hep-ph]].
- [49] S. Dittmaier, M. Krämer and M. Spira, *Phys. Rev. D* **70** (2004), 074010 doi:10.1103/PhysRevD.70.074010 [arXiv:hep-ph/0309204 [hep-ph]].
- [50] S. Dawson, C. B. Jackson, L. Reina and D. Wackerroth, *Phys. Rev. D* **69** (2004), 074027 doi:10.1103/PhysRevD.69.074027 [arXiv:hep-ph/0311067 [hep-ph]].
- [51] C. Duhr, F. Dulat and B. Mistlberger, *Phys. Rev. Lett.* **125** (2020) no.5, 051804 doi:10.1103/PhysRevLett.125.051804 [arXiv:1904.09990 [hep-ph]].
- [52] A. H. Ajjath, A. Chakraborty, G. Das, P. Mukherjee and V. Ravindran, *JHEP* **11** (2019), 006 doi:10.1007/JHEP11(2019)006 [arXiv:1905.03771 [hep-ph]].
- [53] M. A. G. Aivazis, J. C. Collins, F. I. Olness and W. K. Tung, *Phys. Rev. D* **50** (1994), 3102-3118 doi:10.1103/PhysRevD.50.3102 [arXiv:hep-ph/9312319 [hep-ph]].
- [54] R. S. Thorne and R. G. Roberts, *Phys. Rev. D* **57** (1998), 6871-6898 doi:10.1103/PhysRevD.57.6871 [arXiv:hep-ph/9709442 [hep-ph]].
- [55] M. Cacciari, M. Greco and P. Nason, *JHEP* **05** (1998), 007 doi:10.1088/1126-6708/1998/05/007 [arXiv:hep-ph/9803400 [hep-ph]].
- [56] M. Krämer, F. I. Olness and D. E. Soper, *Phys. Rev. D* **62** (2000), 096007 doi:10.1103/PhysRevD.62.096007 [arXiv:hep-ph/0003035 [hep-ph]].

- [57] W. K. Tung, S. Kretzer and C. Schmidt, *J. Phys. G* **28** (2002), 983-996
doi:10.1088/0954-3899/28/5/321 [arXiv:hep-ph/0110247 [hep-ph]].
- [58] R. S. Thorne, *Phys. Rev. D* **73** (2006), 054019 doi:10.1103/PhysRevD.73.054019
[arXiv:hep-ph/0601245 [hep-ph]].
- [59] S. Forte, D. Napoletano and M. Ubiali, *Phys. Lett. B* **751** (2015), 331-337
doi:10.1016/j.physletb.2015.10.051 [arXiv:1508.01529 [hep-ph]].
- [60] M. Bonvini, A. S. Papanastasiou and F. J. Tackmann, *JHEP* **11** (2015), 196
doi:10.1007/JHEP11(2015)196 [arXiv:1508.03288 [hep-ph]].
- [61] M. Bonvini, A. S. Papanastasiou and F. J. Tackmann, *JHEP* **10** (2016), 053
doi:10.1007/JHEP10(2016)053 [arXiv:1605.01733 [hep-ph]].
- [62] S. Forte, D. Napoletano and M. Ubiali, *Phys. Lett. B* **763** (2016), 190-196
doi:10.1016/j.physletb.2016.10.040 [arXiv:1607.00389 [hep-ph]].
- [63] C. Duhr, F. Dulat, V. Hirschi and B. Mistlberger, *JHEP* **08** (2020) no.08, 017
doi:10.1007/JHEP08(2020)017 [arXiv:2004.04752 [hep-ph]].
- [64] D. de Florian *et al.* [LHC Higgs Cross Section Working Group], doi:10.23731/CYRM-2017-002
[arXiv:1610.07922 [hep-ph]].
- [65] See ‘‘https://twiki.cern.ch/twiki/bin/view/LHCPhysics/LHCHWGBBH#NLO_NNLLpart_ybyt_matching’’.
- [66] F. Maltoni, Z. Sullivan and S. Willenbrock, *Phys. Rev. D* **67** (2003), 093005
doi:10.1103/PhysRevD.67.093005 [arXiv:hep-ph/0301033 [hep-ph]].
- [67] E. Boos and T. Plehn, *Phys. Rev. D* **69** (2004), 094005 doi:10.1103/PhysRevD.69.094005
[arXiv:hep-ph/0304034 [hep-ph]].
- [68] F. Maltoni, T. McElmurry and S. Willenbrock, *Phys. Rev. D* **72** (2005), 074024
doi:10.1103/PhysRevD.72.074024 [arXiv:hep-ph/0505014 [hep-ph]].
- [69] F. Maltoni, G. Ridolfi and M. Ubiali, *JHEP* **07** (2012), 022 [erratum: *JHEP* **04** (2013), 095]
doi:10.1007/JHEP04(2013)095 [arXiv:1203.6393 [hep-ph]].
- [70] R. V. Harlander, *Eur. Phys. J. C* **76** (2016) no.5, 252 doi:10.1140/epjc/s10052-016-4093-x
[arXiv:1512.04901 [hep-ph]].
- [71] S. Dittmaier, M. Krämer, A. Muck and T. Schluter, *JHEP* **03** (2007), 114
doi:10.1088/1126-6708/2007/03/114 [arXiv:hep-ph/0611353 [hep-ph]].
- [72] S. Dawson, C. B. Jackson and P. Jaiswal, *Phys. Rev. D* **83** (2011), 115007
doi:10.1103/PhysRevD.83.115007 [arXiv:1104.1631 [hep-ph]].
- [73] S. Dittmaier, P. Häfliger, M. Krämer, M. Spira and M. Walser, *Phys. Rev. D* **90** (2014) no.3, 035010
doi:10.1103/PhysRevD.90.035010 [arXiv:1406.5307 [hep-ph]].
- [74] E. Bagnaschi, H. Bahl, E. Fuchs, T. Hahn, S. Heinemeyer, S. Liebler, S. Patel, P. Slavich,
T. Stefaniak and C. E. M. Wagner, *et al.* *Eur. Phys. J. C* **79** (2019) no.7, 617
doi:10.1140/epjc/s10052-019-7114-8 [arXiv:1808.07542 [hep-ph]].